-RESEARCH PAPER-

International Journal of Mining and Geo-Engineering

IJMGE

IJMGE 58-1 (2024) 39-45

DOI: 10.22059/IJMGE.2023.361953.595083

Application of bipolar electrochemistry to follow electrochemical reactions at the semiconductor-electrolyte interface

Saeide Ahmadi [a], Ahmad Ghorbani [a, *] and Hamid Reza Zare [b]

[a] *Department of Mining and Metallurgical Engineering, Yazd University.*

[b] *Department of Chemistry, Yazd University, Yazd, Iran.*

Article History:

Received: 09 July 2023.

Revised: 08 September 2023.

Accepted: 01 October 2023.

ABSTRACT

The properties of metallic minerals and metallic minerals-electrolyte interface have always been a concern in the induced polarization (IP) geophysical method due to their effects on the IP response. Electrochemical reactions, if carried out, affect the interface characteristics. Hence, the occurrence of the reactions and their effects on the IP signal have been modeled through recent research, but they are not well-known yet. Identifying these matters can help to create more realistic physical and petrophysical models, for a better explanation of IP effects. So, in the present study, 11 metallic mineral samples and the laboratory method named bipolar electrochemistry, introduced for the first time to the IP research field, have been used to show the performance of electrochemical reactions at the interface and the effect of various metallic minerals on them. The results showed that if the applied external electric potential is high enough, electrochemical reactions are carried out at the metallic minerals-electrolyte interface. In this study, these reactions were electrolysis of water and were carried out in all minerals (except sphalerite). However, the potential required to initiate the reactions was different for different minerals. The lack of water electrolysis reaction on the surface of sphalerite can probably be attributed to its non-conductivity. On the other hand, the external potential responsible for the interface reactions was linearly linked to the potential difference between the two sample's extremities. Considering the different potentials required to start the reactions in various samples-electrolyte interfaces, and the absence of these reactions in the case of sphalerite samples, it can be concluded that the samples' compounds affect the reactions and their commencing potentials. So, we believe that by studying these reactions, some properties of the metallic minerals can be achieved. Identifying the minerals' properties and the reactions that can occur at their surfaces is essential for a detailed understanding of the factors affecting the IP phenomenon. To do this, we found bipolar electrochemistry as an appropriate way.

Keywords: *Bipolar electrochemistry, Induced polarization, Redox reactions, Sulfide minerals.*

1. Introduction

The geologic environment is the complex of the solid, liquid, and gaseous phases. The phases' properties and the geometry arrays between them cause the environment's complex characteristics. Usually, the resistivity of solid and gaseous phases is high, so electrolyte conductivity plays the leading role in bulk conductivity and charge transfer in the environment. The polarizable liquid-solid/gaseous interfaces can increase a capacitance component to the environment's electrical properties. The conduction and capacitance components of electric charge can be explained using the complex conductivity conception in the induced polarization (IP) method. IP is a geophysical method applied in the frequency range of a few mHz to several kHz for exploration and environmental purposes. Researchers use the IP models to interpret the IP response. The IP models are constructed to reduce huge IP data sets to limited and meaningful parameters describing the physicochemical properties of subsurface areas (e.g., [1]). In other words, the IP models link the IP response to the physical and chemical processes of the subsurface porous media. So, a sound understanding of these processes is essential for the interpretation of measured IP data.

The IP phenomenon is particularly pronounced in rocks containing metallic particles, such as lead, copper, and gold, semi-metals, such as graphite, and semiconductors, such as some oxide and sulfide metallic minerals (e.g., [2]). These minerals are considered in mineral exploration due to their substantial amounts of economically valuable metals. It has been stated for a long time that the IP phenomenon in metallic minerals is related to electrochemical effects (e.g., [3]). This is generally derived from the fact that the conduction mechanism in the host rock is ionic or electrolytic in nature, while it is fundamentally electronic in a certain group of metallic minerals. Thus, the interface between the metallic minerals and the surrounding electrolyte acts as a barrier to the ions in the electrolyte and the electric charges in the metallic minerals. The charge transfer across this interface is possible only if an electrochemical reaction such as oxidation-reduction (redox) can occur. Hence, the interface has an impedance that depends on the electrochemical reactions and the ions feeding the reactions [3]. However, many of the IP models proposed so far have not considered the electrochemical basics of the impedance of metallic minerals-electrolyte interface (e.g., [4-7]) or the realistic geometry of the metallic minerals. Therefore, these models do not fit well with the measured IP data, and as a result, do not properly evaluate the porous media's petrophysical properties.

* Corresponding author. *E-mail address:* a.ghorbani@yazd.ac.ir (A. Ghorbani).

To overcome these shortcomings, Wong (1979) exposed, in a rather complicated way, an IP model for a suspension of highly conductive spherical particles. His model which was based on the solution of the Poisson-Nernst-Planck (PNP) equations system, has been used as a basic study in newer research. Wong and Strangway (1981) expanded Wong's model for non-spherical particles. Mahan et al. (1986) tested Wong's model on the experimental samples of sand and sulfides. Gurin et al. (2015) and Placencia-Gómez and Slater (2014) simplified Wong's model. They studied the metal particle polarization in the form of dielectric polarization though it was not right to use dielectric conception to discuss metallic particle polarization. Bücker et al. (2018, 2019), using Wong's model, described how electrochemical reactions occur at the metal-electrolyte interface and how these reactions affect the IP response. However, their method was also complicated and could not explain some of the important experimental observations.

Except for the above-mentioned defects of the previous bunch of research, none of them has applied a simple experimental method to observe and analyze the electrochemical reactions that can occur at the metallic minerals-electrolyte interfaces. Also, the role of various metallic minerals in these reactions has not been compared. Therefore, for the first time, we use the bipolar electrochemistry experimental method to conduct such analyses. So, we chose 11 semiconductor samples of pyrite, chalcopyrite, sphalerite, galena, and magnetite from various mineral deposits in Iran, and considered each of them as a bipolar electrode (BPE). Then we immersed them in an electrolyte and made a simplified medium to observe the electrochemical reactions taking place at metallic minerals-electrolyte interfaces, and the role of metallic minerals in these reactions. The results of this study are beneficial for understanding the factors driving the electrochemical reactions at the metallic minerals-electrolyte interface. Likewise, they help find the effects of the metallic minerals on the reactions and recognize the metallic minerals' physicochemical characteristics. These subjects, in turn, help to a detailed understanding of the factors affecting the IP response and a better interpretation of IP data. These matters along with introducing a new way to study the electrochemical reactions at the metallic minerals-electrolyte interface, are innovations of the present study.

2. Materials and Methods

2.1. Bipolar Electrochemistry Principles

In the bipolar electrochemistry, there is a microchannel containing an electrolyte solution. An isolated conductive substance, named bipolar electrode, is placed in the electrolyte, and an external electric field is applied to the set parallel to the BPE length (Fig. 1a). The central point of the microchannel and the bipolar electrode coincide (x0 in Fig. 1b). There is no physical connection between the bipolar electrode and the power supply [14]. Two driving electrodes are located on both sides of the BPE and connected to a DC power supply to apply the external electric field to the bipolar electrode. The driving electrodes are made from an inert conductive material, such as graphite or platinum.

The external electric potential (field) (Etot) applied to the above-mentioned set causes the BPE to float at an equilibrium potential (Eelec). The magnitude of this potential depends on the BPE's position concerning the field and the electrolyte composition. Because the BPE is an equipotential surface, Eelec is the same on its surface. But, due to the existing electric field in the electrolyte, the potential difference at the BPE-electrolyte interface varies along the BPE length. The interfacial potential difference between the BPE and electrolyte (ΔEelec) is highest at the extremities of the bipolar electrode.

ΔE_{elec} is the potential difference between BPE poles [15] and is the fraction of E_{tot} dropped over the BPE [16-18]. It is a critical parameter to analyze the electrochemical processes at BPE [14, 19] and is obtained by Equation 1 [15]:

$$\Delta E_{elec} = E_{tot}\left(\frac{l_{elec}}{l_{channel}}\right) \quad (1)$$

The potential difference corresponds to the anodic and cathodic overpotentials, η_{an} and η_{cat}, which drive the redox reactions at two ends of the BPE (Fig. 1b). When the overpotentials at each end of the BPE reach the values necessary to start the redox reactions, the anodic and cathodic reactions are performed simultaneously at the two poles of the BPE as shown in Figs. 1a and 1b [14-15, 17, 20-21]. The boundary between the BPE anodic and cathodic poles is a point with a zero potential difference concerning the electrolyte (x_0 in Fig. 1b). Although this point is located at the center of the BPE in Fig. 1b, its real position depends on the nature of faradaic currents, which take place at the two BPE poles [16].

The anodic and cathodic overpotentials at the BPE's surface are affected by parameters such as the nature and concentration of components involved in the redox reaction, the pH of the electrolyte solution, the material of the surface of the BPE poles, the position of the BPE and the conductivity of the electrolyte solution [16, 22-25].

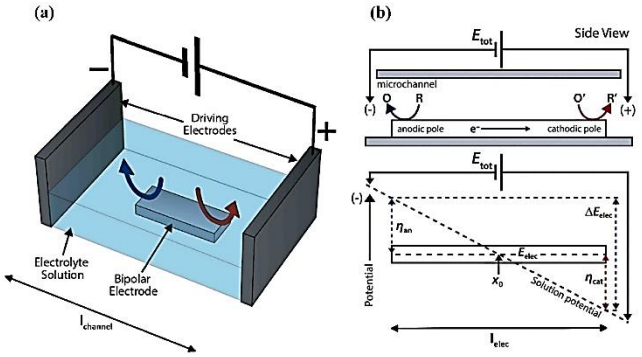

Fig. 1. Schematic representation of the bipolar electrochemistry system. (a) A BPE is located at the center of a microchannel containing an electrolyte solution. Two driving electrodes connected to a DC power supply apply an external electric potential (Etot) to the set (modified from [14-15]). (b) Etot causes the equilibrium potential (Eelec) on the BPE's surface, and anodic and cathodic overpotentials, ηan and ηcat, respectively, at its poles. The overpotentials drive the reduction and oxidation reactions at the poles, red and blue arrows, respectively. The overpotentials are zero at the center of BPE (x0). ΔEelec is the potential difference between the BPE's poles. The driving electrodes' distance (lchannel), and the BPE length (lelec) are displayed in this Figure (modified from [14-15]).

2.2. The Samples and the Measurement Method

The samples for the study were separated from natural rocks which are shown in Fig. 2 and are composed of:

1. Two pieces of sphalerite, S1 and S2, both from one deposit;
2. One piece of magnetite, M1;
3. Three pieces of pyrite, P1 and P2, from one deposit and surrounded by quartz, and P3 from another deposit;
4. Two pieces of chalcopyrite, C1 from one deposit and C2 from another;
5. Three pieces of Galena, G1 and G2, from one deposit and G3 from another.

The characteristics of the samples, including the dimensions (length, width, height, and area) are reported in Table 1.

The study of the samples' polished sections, which can be observed in Fig. 3, showed the mineralogy of the samples:

1. S1 and S2 contain only sphalerite.
2. M1 includes magnetite along with 3% to 4% hematite.
3. P1 and P2 are composed only of one generation of pyrite.
4. P3 includes two generations of pyrite so that the low-value second generation disseminates in the first.
5. C1 consists of chalcopyrite mineral, 10% to 15% pyrrhotite, and 1% to 2% sphalerite.
6. C2 involves chalcopyrite mineral, less than 5% pyrrhotite, and less than 1% disseminated hematite.
7. G1 and G2 consist of only Galena.
8. G3 comprises Galena accompanied by less than 1% pyrite.

Table 1. The Samples' Dimensions, including length (l), width (w), height (h), and area (A).

Sample	l (m)	l.w.h (m^3)	A (m^2)
S1 (Sphalerite)	0.009	0.009×0.005×0.006	0.000045
S2 (Sphalerite)	0.006	0.006×0.006×0.006	0.000036
M1 (Magnetite)	0.009	0.009×0.007×0.006	0.000063
P1 (Pyrite)	0.009	0.009×0.007×0.006	0.000063
P2 (Pyrite)	0.006	0.006×0.005×0.006	0.00003
P3 (Pyrite)	0.006	0.006×0.005×0.006	0.00003
C1 (Chalcopyrite)	0.006	0.006×0.004×0.006	0.000024
C2 (Chalcopyrite)	0.006	0.006×0.006×0.005	0.000036
G1 (Galena)	0.009	0.009×0.006×0.006	0.000054
G2 (Galena)	0.006	0.006×0.006×0.006	0.000036
G3 (Galena)	0.006	0.006×0.006×0.006	0.000036

Fig. 2. 11 samples are separated from the metal ores illustrated in the Figure and used in bipolar electrochemistry experiments. S1 and S2: sphalerite, M1: magnetite, P1 to P3: pyrite, C1 and C2: chalcopyrite, and G1 to G3: galena. The characteristics of the samples are reported in Table 1. The polished section of the samples was prepared and studied (see, Fig. 3).

All preparations and studies of the polished sections were performed at Yazd University, Department of Mining and Metallurgical Engineering, Thin and Polished Sections Laboratory. Then, the electrochemical experiments and measurements were carried out at Yazd University, Department of Chemistry.

For the experiment, a DC power supply model OWON P4603/ 60V/ 3A (Fig. 4a) was used. An electrochemistry cell with dimensions 10×5×5 cm was made from Plexiglas (Fig. 4b). Then, the brine with conductivity (σ_w) 0.13 Siemens/meter was prepared.

To do this, 99.99% pure NaCl and distilled water were used to provide a 0.01 molar electrolyte. The bromothymol blue indicator was added to the electrolytes to observe the redox reaction onset at the sample-electrolyte interface. Bromothymol blue is a pH indicator and is utilized to identify weak acids and bases. It is mostly used in applications that would have a relatively neutral pH (near 7). The indicator turns to green, yellow, and blue colors in the neutral, acidic, and alkaline solutions, respectively.

Afterward, one of the samples, serving as a BPE, was placed in the cell (Fig. 4a). The middle points of the sample and cell coincided. Two graphitic electrodes, as the driving electrodes, were located at a distance of 5 cm and immersed in the electrolyte (Fig. 4a). No substances or devices were attached to the electrolyte and BPE set, except driving electrodes. The lack of direct connection between the BPE and the power supply is the similarity of the bipolar electrochemistry system with the media considered in the IP method. The driving electrodes were connected to a 60-volt DC power supply.

Then, the external electric potential was applied to the cell through the driving electrodes and increased gradually until the redox reactions were observed at two poles of the sample according to the color change of bromothymol blue.

At this point, the required external potential that must be applied to the feeder electrodes to perform the redox reactions on the two BPE poles was recorded. This procedure was repeated for all samples. The samples and all the instruments were rinsed with distilled water before entering the electrolyte.

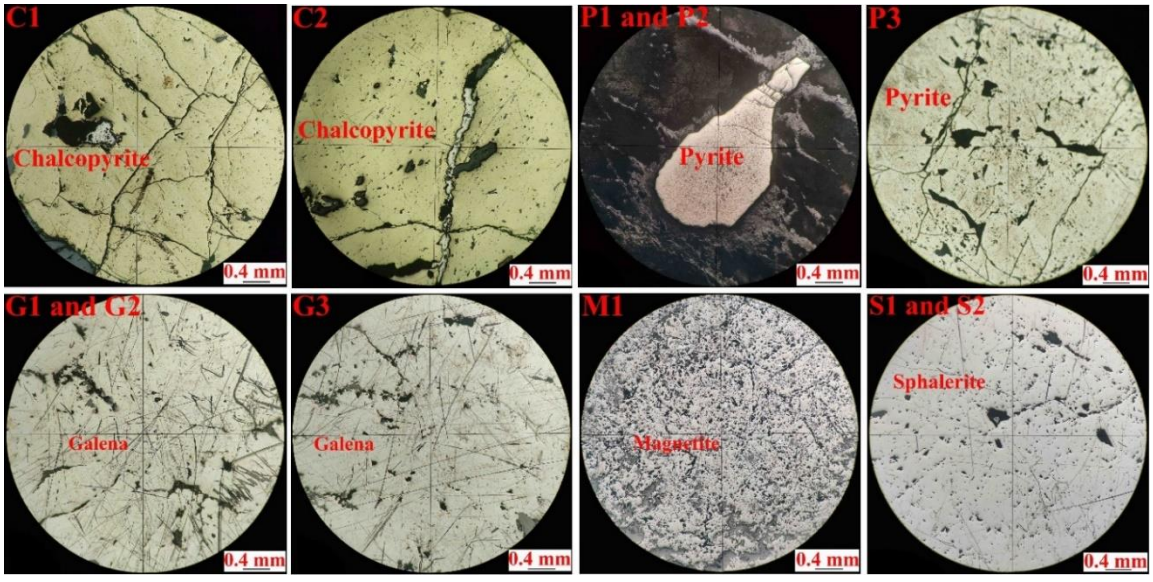

Fig. 3. The polished section of the samples. Based on the close similarity between P1 and P2, G1 and G2, and S1 and S2, one of them is illustrated in this Figure.

3. Results and Discussion

As mentioned before, applying a sufficiently uniform external electric field across the electrolyte results in the electrochemical reactions at the BPE's poles. In the absence of the BPE, an ionic current flow between the driving electrodes. When the BPE is immersed in the electrolyte, the potential distribution changes in a way that the highest potential difference between the BPE and the electrolyte is shaped at the two

BPE's extremities. In agreement with this, the bromothymol blue color was observed changing just at two poles of each sample after applying high enough external electric potential. This color change identified that the electrochemical reactions were driven at the sample-electrolyte interface. We believe that the electrochemical reactions at our samples-electrolyte interface were oxidation and reduction of water. Because the color changing of bromothymol blue is the same at both poles of all samples and these reactions are accompanied by hydrogen and oxygen bubbles at the cathodic and anodic poles, respectively. In fact, the bromothymol blue turned blue at the cathodic pole due to producing OH^- and became yellow at the anodic pole owing to producing H^+ (Equations 2 and 3) (see, for instance, [15, 23]).

$$H_2O+e^- \rightarrow OH^- + \frac{1}{2}H_2 \quad E^0_{\text{cathodic (pH=7)}} = -0.613 \text{ (Volt)} \tag{2}$$

$$H_2O \rightarrow \frac{1}{2}O_2 + 2H^+ + 2e^- \quad E^0_{\text{anodic (pH=7)}} = +1.517 \text{ (Volt)} \tag{3}$$

Carrying out the electrochemical reactions at the pyrite (P1)-electrolyte interface is illustrated in Fig. 5 and for the other samples in Fig. 6.

The electrochemical reactions were also observed at the graphitic driving electrodes but did not affect our BPEs (e.g. [15]). That is because the graphitic driving electrodes are inert and do not participate in any electrochemical reaction. These electrodes induce potential to the BPE and as a result, perform electrochemical reactions at both ends of the BPE.

Another point is that the electrochemical reactions were not observed for sphalerite, even with the ultimate potential produced by the power supply (60 V). The difference between sphalerite and the other samples in this study is in their conductivity. So that the sulfide minerals' conductivity, except for sphalerite, varies from 7×10^{-3} to 9×10^{6} S/m and in the case of oxide minerals, it is in the range of 5×10^{-8} to 9×10^{4} S/m. While the sphalerite's conductivity varies from 10^{-8} to 0.95 S/m and it is an insulator at ordinary temperatures [26-28]. The conductivity of pyrite is variable and has been reported from 0.1 to 10000 S/m in [26] and equals 4800 S/m in [29]. The conductivity of chalcopyrite varies in a wide range and has been stated as 2900 S/m in [30]. The conductivity of galena has been reported from 1000 to 10000 S/m [31] and for magnetite, it ranges from 10 to 1000 S/m [32]. Hence, despite the other samples, the potential difference at the sphalerite-electrolyte interface did not reach the necessary level to commence the electrochemical reactions probably due to sphalerite's very low conductivity.

The experimental E_{tot} required to commence the reactions at each sample is reported in Table 2. With the experimental E_{tot}, $l_{channel}$, and l_{elec} in hand, the ΔE_{elec} can be calculated for all samples (Table 2). It can be observed in Fig. 7 that there is a linear relationship between ΔE_{elec} and E_{tot} for all samples. It means the potential difference between two samples' poles is linearly dependent on the external potential applied to the whole set. This is an important point that we utilize to conclude that if E_{tot} is high enough, the sample can be an electronic path for external electric current and the electrochemical reactions take place between the sample and electrolyte (see, for instance, [33]). Duval et al. (2003b) have also observed that the electrochemical process is occurring at the gold interface owing to the reduction and oxidation of the water on both sides. While this process is carried out at the aluminum-electrolyte interface due to the reduction of water on the cathodic side and the dissolution of the metallic phase on the other. However, it is beyond the scope of this study and will be researched in our future studies. It should be noted that the potentials required for the electrolysis of water at the metallic minerals' poles mentioned in Table 2 are different from the values mentioned for the electrolysis of water in Equations 2 and 3.

This is a common phenomenon, so that depending upon the type of bipolar electrode, the electrolysis of water might be observed at the different potentials rather than the ones mentioned in the equations. So far, two observations have indicated that the mineral's type affects the electrochemical reactions at the mineral-electrolyte interface, including the different commencing potential, and the lack of the reactions in the case of sphalerite samples. In our experiments, all the parameters except the samples' composition and length remained constant.

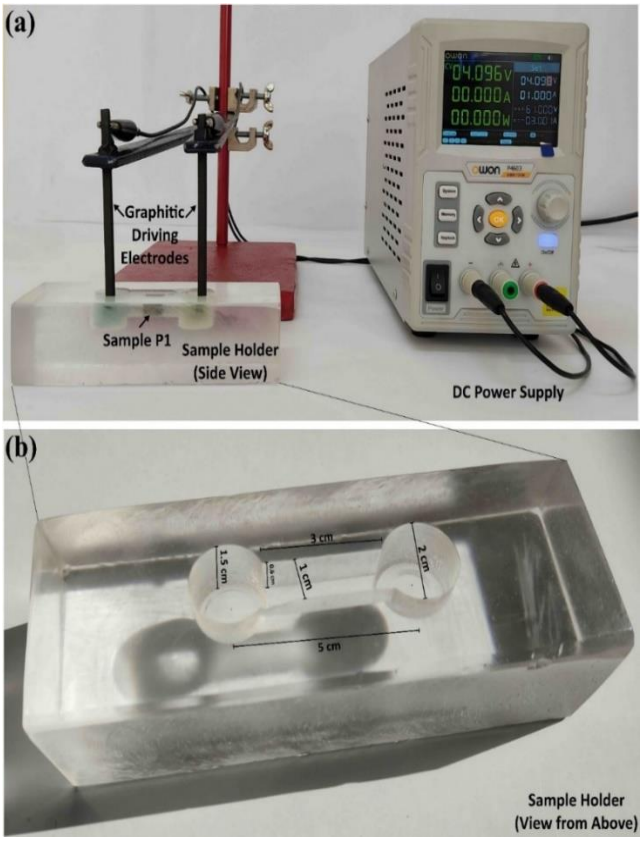

Fig. 4. The representation of a) the measurement setup, including DC power supply, cables, sample holder, and graphitic driving electrodes. b) Showing the sample holder with its dimensions.

However, the difference between the required potential leading to electrochemical reactions is observed even in the case of different samples with the same length, e.g., P1 (pyrite), G1 (Galena), and M1 (magnetite) with 0.9 cm length, likewise for the other samples. So, it seems the composition's effect on the commencing potential is more significant than the length. In agreement with our results, Duval et al. (2001, 2003b) also observed these different potentials for the cases of aluminum, chromium, and gold electrodes. Duval et al. (2003a) demonstrated that the potential difference beyond which the redox reactions take place is not the same in the case of aluminum and gold BPEs. Fosdick et al. (2013) also attributed different required external electric potentials for diverse electroactive materials to their different standard potential.

Our observations represent that it is possible to understand the interactions between the metallic minerals and the electrochemical reactions at the mineral-electrolyte interfaces using the bipolar electrochemistry method that provides an environment similar to the porous media of interest in the IP method. These interactions will certainly help recognize the metallic minerals' physicochemical properties and the effective factors leading to electrochemical reactions at their surfaces. These are important parameters affecting the IP signal. So, one of the most important subjects that will be investigated in the future research is the relation between the external electric potential required to start the reactions and the percentage of the metallic minerals' electroactive elements. The aforementioned elements are crucial for driving the faradaic currents between the metallic minerals and their surrounding electrolyte. These currents have a considerable effect on the IP response (see for instance, [8]). In fact, the present study was considered as the first attempt to develop a tangible method, in contrast to previous research in this field, to investigate the interactions between metallic minerals and the electrochemical reactions at the mineral-electrolyte interface.

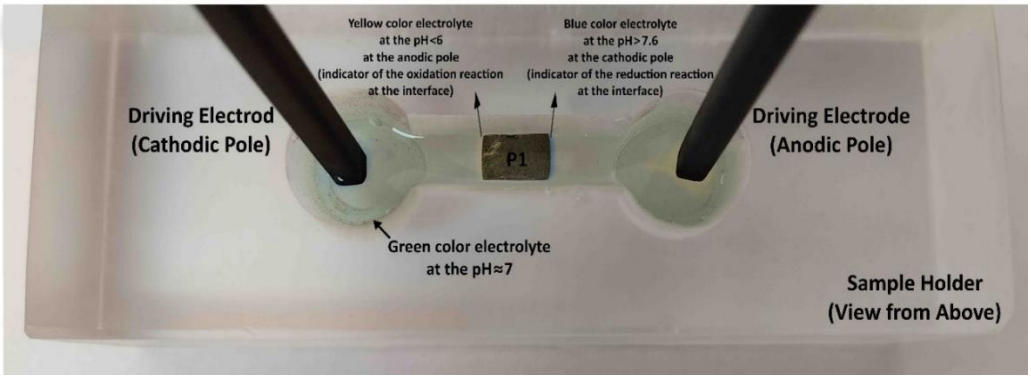

Fig. 5. The representation of the beginning of the electrochemical reactions at the pyrite-electrolyte interface using the bipolar electrochemistry system. The driving electrodes' distance and the length of the pyrite sample are 5 and 0.9 cm, respectively. The bromothymol blue indicator was added to the electrolyte to observe the electrochemical reactions at the pyrite-electrolyte interface. The blue color of the indicator on the right side of the sample determines the reduction reaction at the cathodic pole of the pyrite particle (producing OH^-). The yellow color of the indicator at the left side of the pyrite particle specifies the oxidation reaction at the anodic pole of the sample (producing H^+). The electrochemical reactions occurred at the graphitic driving electrodes, but they did not affect the sample.

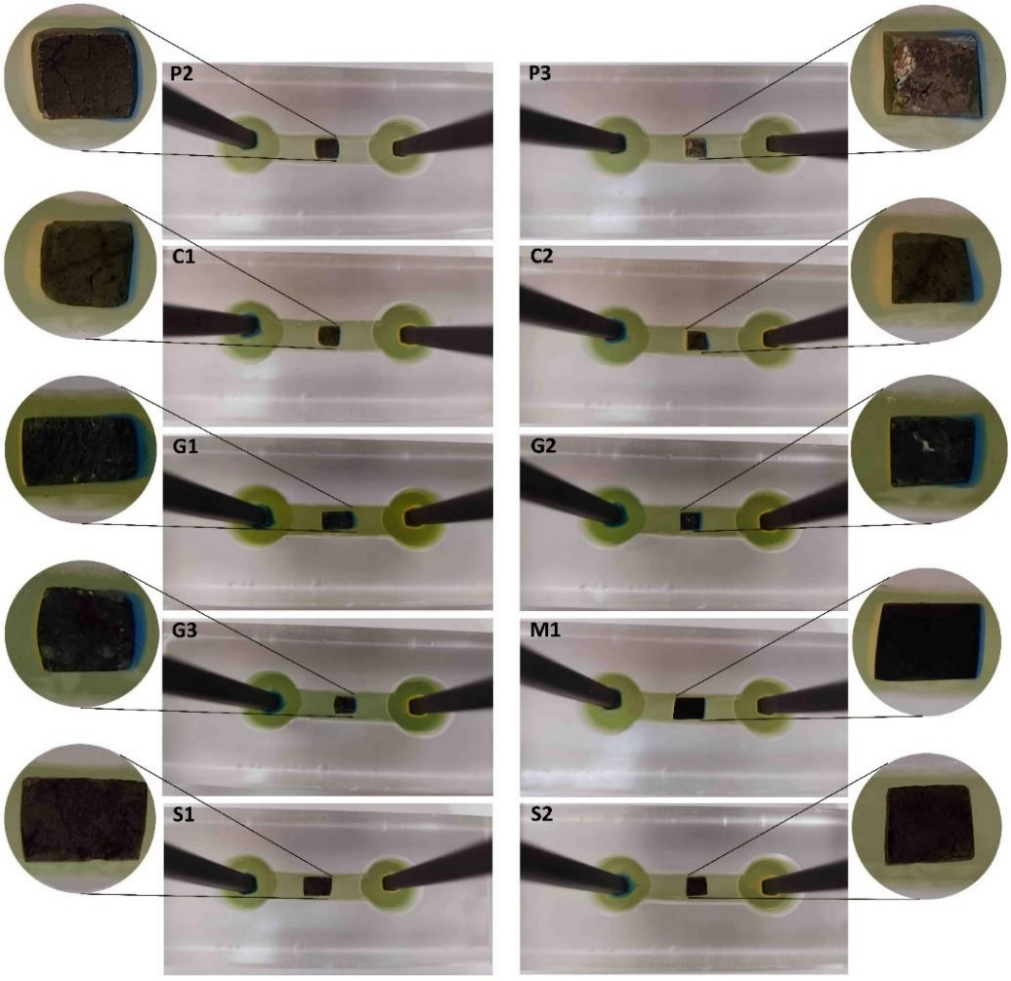

Fig. 6. The representation of driving the electrochemical reactions at all samples-electrolyte interfaces, except P1, using the bipolar electrochemistry system. The electrochemical reactions were not observed at sphalerite even with the ultimate electric potential of the DC power supply.

4. Conclusions

In this research, as an interdisciplinary study, for the first time, the bipolar electrochemistry method has been introduced as a way to simulate the media around the metallic minerals studied in the induced polarization geophysical method. And using it, the occurrence of electrochemical reactions at the metallic minerals-electrolyte interface and the minerals' effect on the reactions has been observed. Based on our observations, the sufficiently high external potential carries out the reactions at the interface. This potential varies for different minerals

even with the same lengths and it is linearly related to the potential difference between two metallic minerals' extremities. In addition, despite using the high external potential, no electrochemical reactions were observed at the sphalerite interface. Unlike other minerals investigated in this study, sphalerite is a non-conductive semiconductor. Probably because of that, the external potential has not been able to generate enough potential difference between sphalerite and electrolyte to carry out electrochemical reactions at the interface. As, in our experiments, all the factors, except the mineral's type and length, hold steady, the observations were attributed for the potential required to initiate the reactions and the lack of their occurrence in the case of sphalerite to the minerals' physicochemical properties.

Table 2. The experimental parameters E_{tot} and ΔE_{elec} to commence the electrochemical reactions at the samples' poles in electrolyte with the conductivity of 0.13 S/m. To prepare the brine with this conductivity, we used pure NaCl and distilled water and provided a 0.01 molar electrolyte.

Sample	σ_w (S/m) = 0.13	
	E_{tot} (Volt)	ΔE_{elec} (Volt)
S1 (Sphalerite)	60	undefined
S2 (Sphalerite)	60	undefined
M1 (Magnetite)	8.50	1.53
P1 (Pyrite)	4.70	0.846
P2 (Pyrite)	7.75	0.93
P3 (Pyrite)	7.80	0.936
C1 (Chalcopyrite)	6.40	0.768
C2 (Chalcopyrite)	3.90	0.468
G1 (Galena)	15.90	2.862
G2 (Galena)	6.90	0.828
G3 (Galena)	5.10	0.612

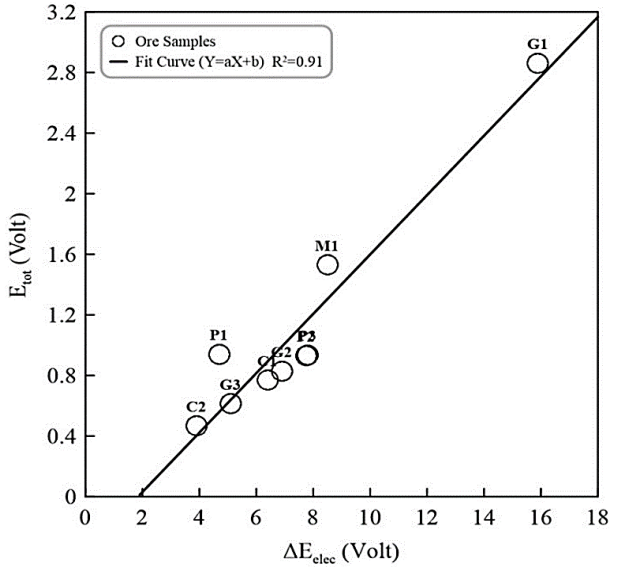

Fig. 7. The linear relationship between ΔE_{elec} and E_{tot} for all samples. The black line is the linear fit on the samples.

So, we showed with a simple experiment that depending on the value of the applied external potential and the metallic mineral's type, the electrochemical reactions can take place at the metallic minerals-electrolyte interface The Bipolar electrochemistry is a suitable method to study the interactions between metallic minerals and the probable electrochemical reactions at the minerals-electrolyte interfaces and is useful for a better understanding of the factors affecting the IP response.

Acknowledgment

The authors are grateful to Dr. Seyed Hossein Mojtahedzade, associate professor of mining engineering at Yazd University, for studying the polished sections of our samples. We also thank Dr. Abolfazl Naser-Sadrabadi, who significantly contributed to conducting laboratory experiments.

REFERENCES

[1] Bücker, M. (2018). Pore-scale modelling of induced-polarization mechanisms in geologic materials. Doctoral dissertation. Bonn, University of Bonn. https://d-nb.info/118557610X/34.

[2] Pearce, C. I., Pattrick, R. A., & Vaughan, D. J. (2006). Electrical and magnetic properties of sulfides. Reviews in Mineralogy and Geochemistry, 61(1), 127-180. https://doi.org/10.2138/rmg.2006.61.3.

[3] Wong, J. (1979). An electrochemical model of the induced-polarization phenomenon in disseminated sulfide ores. Geophysics, 44(7), 1245-1265. https://doi.org/10.1190/1.1441005.

[4] Wait, J. R. (1959). A phenomenological theory of over-voltage for metallic particles, in Over-voltage research and geophysical applications. J. R. Wait, Ed., New York, Pergamon Press.

[5] Madden, T. R., & Marshal, D. J. (1959). Induced polarization: a study of its causes and magnitudes in geologic materials. A.E.C. rep. RME-3160.

[6] Madden, T. R., & Cantwell, T. (1967). Induced polarization: a review. Mining Geophysics, 2, SEG, Tulsa.

[7] Loeb, J. (1969). Sur la nature nhvhico-chimiuue de 1a polarization provoquee. Rev. de l'Inst. Francais des Petrole et Ann. Des Combustibles Liquides, 24, 1455-1476.

[8] Wong, J., & Strangway, D. (1981). Induced polarization in disseminated sulfide ores containing elongated mineralization. Geophysics, 46(9), 1258-1268. https://doi.org/10.1190/1.1441264.

[9] Mahan, M. K., Redman, J. D., & Strangway, D. W. (1986). Complex resistivity of synthetic sulphide bearing rocks. Geophysical Prospecting, 34(5), 743-768, https://doi.org/10.1111/j.1365-2478.1986.tb00491.x.

[10] Gurin, G., Titov, K., Ilyin, Y., & Tarasov, A. (2015). Induced polarization of disseminated electronically conductive minerals: A semi-empirical model. Geophysical Journal International, 200(3), 1555-1565. https://doi.org/10.1093/gji/ggu490.

[11] Placencia-Gómez, E., & Slater, L. D. (2014). Electrochemical spectral induced polarization modeling of artificial sulfide-sand mixtures. Geophysics, 79(6), EN91-EN106. https://doi.org/10.1190/geo2014-0034.1.

[12] Bücker, M., Flores Orozco, A., & Kemna, A. (2018). Electrochemical polarization around metallic particles- Part 1: The role of diffuse-layer and volume-diffusion relaxation. Geophysics, 83(4), 1-53. https://doi.org/10.1190/geo2017-0401.1.

[13] Bücker, M., Undorf, S., Flores Orozco, A., & Kemna, A. (2019). Electrochemical polarization around metallic particles- Part 2: The role of diffuse surface charge. Geophysics, 84(2), e57-e73. https://doi.org/10.1190/geo2018-0150.1.

[14] Crooks, R. M. (2016). Principles of Bipolar Electrochemistry. ChemElectroChem, 3(3), 357-359. https://doi.org/10.1002/celc.201500549.

[15] Fosdick, S. E., Knust, K. N.; Scida, K., & Crooks, R. M. (2013). Bipolar electrochemistry. Angewandte Chemie International Edition, 52(40), 10438-10456. https://doi.org/10.1002/anie.201300947.

[16] Duval, J., Kleijn, J. M., & van Leeuwen, H. P. (2001). Bipolar electrode behaviour of the aluminum surface in a lateral electric field. Journal of Electroanalytical Chemistry, 505(1-2), 1-11. https://doi.org/10.1016/S0022-0728(01)00461-2.

[17] Mavré, F., Anand, R. K., Laws, D. R., Chow, K.-F., Chang, B.-Y., Crooks, J. A., & Crooks, R. M., (2010). Bipolar electrodes: a useful tool for concentration, separation, and detection of analytes in microelectrochemical systems. Analytical Chemistry, 82(21), 8766-8774. https://doi.org/10.1021/ac101262v.

[18] Zhan, W., Alvarez, J., & Crooks, R. M. (2002). Electrochemical sensing in microfluidic systems using electrogenerated chemiluminescence as a photonic reporter of redox reactions. Journal of the American Chemical Society, 124(44), 13265-13270. https://doi.org/10.1021/ja020907s.

[19] Shida, N., & Inagia, S. (2020) Bipolar electrochemistry in synergy with electrophoresis: Electric field-driven electrosynthesis of anisotropic polymeric materials. Chemical Communications, 56(92), 14327-14336. https://doi.org/10.1039/D0CC06204A.

[20] Koefoed, L., Pedersen, S. U., & Daasbjerg, K. (2017). Bipolar electrochemistry–a wireless approach for electrode reactions. Current Opinion in Electrochemistry, 2(1), 13-17. https://doi.org/10.1016/j.coelec.2017.02.001.

[21] Wang, Y. L., Cao, J. T., & Liu, Y. M. (2022) Bipolar Electrochemistry– A powerful tool for micro/nano electrochemistry. Chemistry Open, 11(12), e202200163. https://doi.org/10.1002/open.202200163.

[22] Duval, J. F. L., Huijs, G. K., Threels, W. F., Lyklema, J., & van Leeuwen, H. P. (2003a). Faradaic depolarization in the electrokinetics of the metal-electrolyte solution interface. Journal of Colloid and Interface Science, 260(1), 95-106. https://doi.org/10.1016/S0021-9797(02)00134-0.

[23] Duval, J. F. L., Minor, M., Cecilia, J., & van Leeuwen, H. P. (2003b). Coupling of Lateral Electric Field and Transversal Faradaic Processes at the Conductor/Electrolyte Solution Interface. The Journal of Physical Chemistry B, 107(17), 4143-4155. https://doi.org/10.1021/jp022459g.

[24] Duval, J. F. L., van Leeuwen, H. P., Cecilia, J., & Galceran, J. (2003c). Rigorous analysis of reversible faradaic depolarization processes in the electrokinetics of the metal/electrolyte solution interface. The Journal of Physical Chemistry B, 107(28), 6782-6800. https://doi.org/10.1021/jp030278o.

[25] Mavré, F., Chow, K.-F., Sheridan, E., Chang, B.-Y., Crooks, J. A., & Crooks, R. M. (2009). Theoretical and experimental framework for understanding ECL emission at bipolar electrodes. Analytical Chemistry, 81(15), 6218-6225. https://doi.org/10.1021/ac900744p.

[26] Parasnis, D. S. (1956). The electrical resistivity of some 'sulphide and oxide minerals and their ores. Tenth Meeting of the European Association of Exploration Geophysicists. held in Hamburg, May 16-18 1956, Sweden. https://doi.org/10.1111/j.1365-2478.1956.tb01409.x.

[27] Dentith, M., & Mudge, S. T. (2014). Geophysics for the mineral exploration geoscientist. Cambridge University Press. New York, ISBN 978-0-521-80951-1 Hardback.

[28] Shuey, R. T. (1975). Semiconducting ore minerals. Elsevier Science Publishers Coy. eBook ISBN: 9780444601421.

[29] Abraitis, P. K., Pattrick, R. A. D., & Vaughan, D. J. (2004). Variations in the compositional, textural and electrical properties of natural pyrite: a review. International Journal of Mineral Processing, 74(1-4), 41-59, https://doi.org/10.1016/j.minpro.2003.09.002.

[30] Mukherjee, S., Ramakrishnan, A., Chen, K. H., Chattopadhyay, K., Suwas, S., & Mallik, R. C. (2019). Tuning the Thermoelectric Properties of Chalcopyrite by Co and Se Double Substitution. AIP Conference Proceedings 2115, 030574 (2019); https://doi.org/10.1063/1.5113413.

[31] Emerson, D. (2017). Conductivities of Broken Hill Style Lead Ores. Preview, 188, 37-40, https://doi.org/10.1071/PVv2017n188p37.

[32] Vella, L., & Emerson, D. (2012). Electrical Properties of Magnetite- and Hematite-Rich Rocks and Ores. 22nd International Geophysical Conference and Exhibition, 26-29 February 2012- Brisbane, Australia.

[33] Naser-Sadrabadi, A., & Zare, H. R. (2019). A highly-sensitive electrocatalytic measurement of nitrate ions in soil and different fruit vegetables at the surface of palladium nanoparticles modified DVD using the open bipolar system. Microchemical Journal. 148, 206-213. https://doi.org/10.1016/j.microc.2019.04.067.C. Zheng et al., "Mineral prospectivity mapping based on Support vector machine and Random Forest algorithm – A case study from Ashele copper–zinc deposit, Xinjiang, NW China," Ore Geol Rev, vol. 159, p. 105567, Aug. 2023, doi: 10.1016/j.oregeorev.2023.105567.